Experimental and Theoretical Studies of Metal Cation−Pyridine Complexes Containing Cu and Ag

Yuh-Sheng Yang, Wen-Yi Hsu, Hsiu-Fang Lee, Ya-Chien Huang, and Chen-Sheng Yeh*

Department of Chemistry, National Cheng Kung University, Tainan, Taiwan 701, R.O.C

Ching-Han Hu*,†

Department of Chemistry, National Changhua University of Education, Changhua, Taiwan, 50058 R.O.C.

Received: May 20, 1999; In Final Form: July 28, 1999

Photodissociative experiments were performed on $Cu^+-C_5H_5N$ and $Ag^+-C_5H_5N$ complexes in the gas phase. The dissociative ligand-to-metal charge-transfer fragments, pyridine$^+$, were observed for both complexes. Photodissociation spectra were recorded as a function of laser wavelength. Two continuous, structureless bands were investigated in each complex. Because of the low-energy ^2D state of the Cu atom, the Cu^+-pyridine dissociative process is more complicated. Several possible mechanisms for this process have been discussed. The binding energies were determined experimentally to be 65.5 and 45.2 kcal/mol for Cu^+-pyridine and Ag^+-pyridine, respectively. $M^+-C_5H_5N$ (M = Cu or Ag) complexes also were studied theoretically using the HF, MP2, and B3LYP methods. All complexes under study show C_{2v} symmetry. The binding energies predicted from the theoretical calculations were less than the experimental values, which were derived from the onset of the charge-transfer appearance combined with the IP (ionization potential). The complexes containing Cu^+ and Ag^+ are characterized predominantly by electrostatic interactions.

Introduction

Gas-phase studies of metal ion−molecule complexes have provided a wealth of valuable information on binding energies, geometries, and the microscopic behavior of chemical and physical processes. Such information is critical to the understanding of heterogeneous catalysis, organometallic reactions in condensed phase, and electron transfer involved in biological systems.[1−4] In addition to experimental investigations, theoretical studies have characterized detailed interactions between metal ions and molecules as well as provided binding energies. For calibration of experimental measurements, several theoretical methods (namely, HF, MP2, and density functional theory) were applied in an attempt to approach accurate values and to establish trends in the metal ion−ligand systems.[5−9]

Experimental techniques such as photodissociation, collision-induced dissociation, and high-pressure equilibrium reactions were employed to establish binding energies. During photodissociation, a fascinating process called dissociative intramolecular charge transfer was observed. The upper limit of the ground-state complex dissociation energy can be deduced from the onset of the charge-transfer appearance combined with the IP (ionization potential) difference between the metal and ligand. Duncan and co-workers have used this method to obtain the dissociation energies of the ground states in metal cation−benzene complexes.[10,11] It should be noted that an accurate binding energy can be acquired only when the threshold is near the dissociation limit of the ground state. In this report, photodissociation also was introduced to investigate ligand-to-metal charge-transfer transitions. Whereas charge-transfer behavior has been observed for ion−molecule complexes, ion clusters, and organometallic species in either gas or solution phases,[10−15] so far benzene and toluene are the only molecules in the metal ion−aromatic ligand complexes to exhibit dissociative charge transfer. Many studies have sought to understand the interaction of the metal bound to the delocalized π-electrons of the aromatic ring.[3,5,7,8,10,11,16] Recently, this mode of binding was found to contribute significantly to biological structures.[3] The π systems provide recognition sites to compete with other electron-rich functional groups, such as −NH and −OH, for metal cations.

Pyridine (C_5H_5N), an azabenzene, is an aromatic molecule consisting of a π-electron ring and a nitrogen atom. Interestingly, very few studies pertaining to the gas-phase interactions of the metal ions with pyridine molecules have appeared thus far. The only published results have been the formation of Ag^+-(pyridine)$_n$ with n = 2, 3, or 4 through gas-phase clustering reactions by Castleman.[17] The binding energies of the third and fourth pyridines attached to Ag^+ were deduced from the van't Hoff plot. However, the detailed interaction, geometry, and binding energy of bare Ag^+ interacting with one pyridine molecule remain unknown. Mulliken noted that pyridine can be treated as a π-type complex or as a σ-donor-type ligand because of the lone-pair electrons on its nitrogen atom.[18] Because conjugation between a lone pair and the π electrons of an aromatic ring has rendered nitrogen the favored basic site, it is reasonable to expect metal cations to orient themselves toward the N atom. The electrostatic model predicts that the metal ions are likely to align with pyridine dipole moment (2.19 D),[19] which is along the C_2 axis. Because the lone-pair electrons and dipole moment coexist on the same plane and in the same direction, electron donation from pyridine to metal ions may be important for the pyridine complexes as well. Henson has theoretically studied Co(acacen)(pyridine) and Co(salen)(pyridine) complexes and shown that the nitrogen of the pyridine is bound to Co atoms.[9]

* To whom correspondence should be addressed. E-mail: csyeh@mail.ncku.edu.tw. Fax: +886-6-2740552.

† E-mail: chingkth@cc.ncue.edu.tw. Fax: +886-4-7211190.

10.1021/jp991662h CCC: $18.00
Published on Web 12/07/1999

Recently, we have experimentally observed the charge-transfer process of Ag^+−pyridine.[20] In this report, we have extended our experimental work to Cu^+−pyridine and have performed theoretical studies of Cu^+ and Ag^+ metal−pyridine complexes. The mechanisms of the dissociative charge transfer and the interactions between metal ions and pyridine are discussed below. Binding energies and structures also are presented and analyzed herein.

Experimental Section

The laser ablation technique combined with a supersonic molecular beam was employed to generate metal cations (Cu^+, Ag^+)−pyridine complexes. The rotating and translating metal rods were irradiated using 532 nm wavelength of the second harmonic output of a Nd:YAG laser (Quantel Brilliant) operated at 10 Hz with 2 mJ/pulse. The pyridine vapor (20.7 Torr at 25 °C)[19] was seeded in helium carrier gas with a back pressure of 6 atm through a 0.75 mm diameter Jordan valve nozzle. The metal ion−pyridine complexes were formed in the cluster source with or without a growth channel, which would have confined the metal plasma to enhance the complexation and condensation.

The ion products were then expanded and skimmed (1 mm diameter) into a reflectron time-of-flight mass spectrometer (R. M. Jordan Company). The positive ions were extracted by applying pulsed voltages to two metal plates, i.e., repeller and extraction plates. To isolate the metal ion complexes with a single pyridine, two parallel plates serving as a mass gate were located inside the flight tube. When the desired ion packet reached the mass gate, the positive voltage was pulsed to ground for ions to pass through and travel along the field-free tube. Complex ions were then reflected by a double-stage reflector and detected using a dual microchannel plate detector. For photodissociation experiments, the dissociation laser beam crossed the selected ion beam at the turning point in the reflector. The fragment and parent ions were analyzed by their times of flight.

Photodissociation action was accomplished by doubling the frequency of a tunable dye laser (Continuum ND6000) pumped by the second or third harmonic of a Nd:YAG pulsed laser (Continuum Surelite). The wavelength-dependent spectrum was obtained by monitoring the intensity of the pyridine fragments as a function of the dissociation laser wavelength. The laser fluence was kept at 2 mJ/cm^2 throughout the experiments.

Theoretical Computations

For metal ion−molecule complexes, it has been shown that the systems with essentially electrostatic interactions can be well described at the SCF level.[21,22] In this study, however, electron correlation effects need to be included because of possible electron donation between transition metals and the ligand. Second-order Møller−Plesset perturbation theory (MP2) and density functional theory/Hartree−Fock hybrid functional theory (B3LYP) were performed on M^+−pyridine (M = Cu or Ag). The SCF method was also carried out for the purpose of comparison.

The geometries of pyridine and pyridine complexes containing metal ions were optimized using several basis sets, i.e., 6-31G, 6-31+G, 6-31G(d), and 6-31G(d,p) for C, H, and N. The double-ζ valence basis sets and the effective core potentials (ECPs) of Hay and Wadt were used for Cu and Ag atoms.[23] The relativistic effects were included in the Hay−Wadt ECPs of Ag. We also added the f polarization functions to increase the flexibility of the ECP basis.[24] It has been found that the inclusion of the f polarization enhanced binding energies at the electron-correlated MP2 level.[7] The f exponents are 3.525 for Cu and 1.611 for Ag.[24] The geometries were fully optimized at the HF, MP2, and B3LYP levels of theories. Harmonic vibrational frequencies were computed at the HF level. These frequencies were scaled by 0.89 and were used in the zero-point energy corrections. The calculations were performed using a Gaussian 98 software package.[25] Natural charge populations were carried out by natural bond orbital (NBO) analysis.

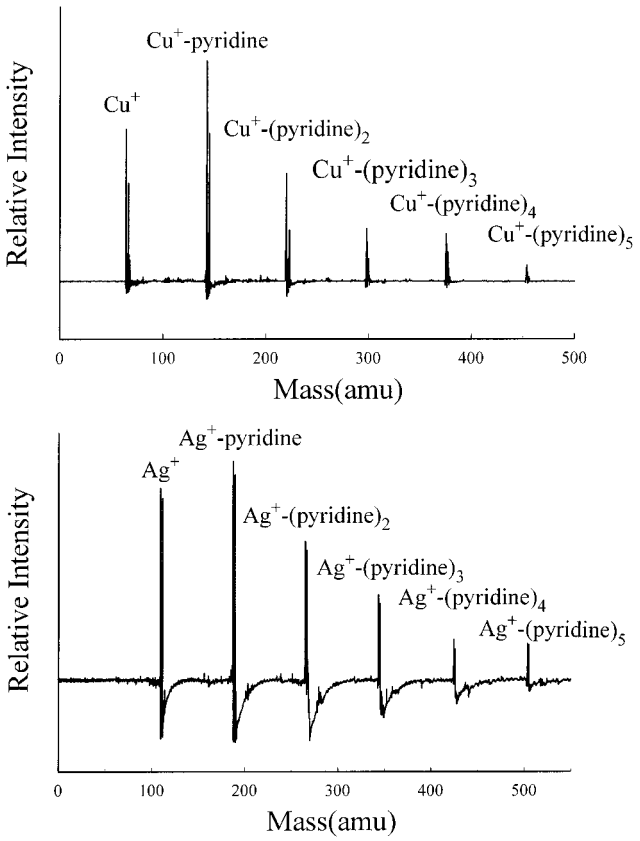

Figure 1. Time-of-flight mass distributions of Cu^+−(pyridine)$_n$ and Ag^+−(pyridine)$_n$. Both spectra were acquired under different intensity scales.

Results and Discussion

Charge-Transfer Process. Figure 1 represents the typical mass distributions of Cu^+−(pyridine)$_n$ and Ag^+−(pyridine)$_n$ complexes, where $n = 0-5$. For both complexes, up to five pyridine molecules coupled to metal ions were generated. The number of complex ions can be controlled by adjusting the experimental conditions, such as the growth channel used in the beam source. As mentioned earlier, the complex ions can be produced with or without a growth channel existing in the cluster source. In the mass spectra, some of the complex peaks display a doublet pattern. This is due to the isotopes of Cu (63, 65) and Ag (107, 109). Once the pyridine vapor was removed from the He carrier gas, these prominent features disappeared immediately. Thus, the pyridine complexes containing metals were synthesized in our source. With the same experimental conditions, we found that copper−pyridine complex ions exhibited larger intensities than those of Ag^+−(pyridine)$_n$. This observation suggested stronger interactions between copper and pyridine, which will be discussed later.

We chose to study the photochemistry of the complexes with only one pyridine. The photodissociative mass spectra are accumulated on the basis of a data acquisition cycle; the ion intensity of the photodissociation laser when on was subtracted

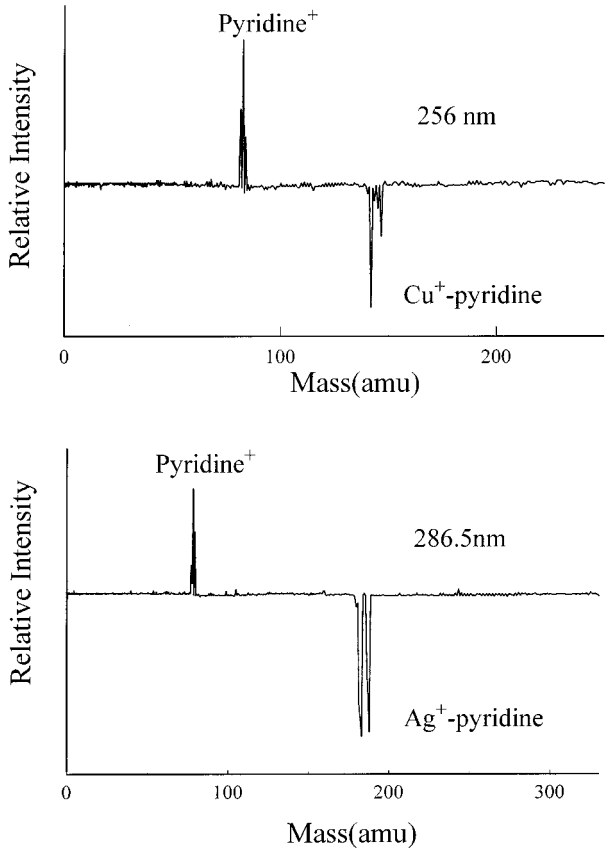

Figure 2. Photodissociation mass spectra of Cu^+−pyridine (256 nm) and Ag^+−pyridine (286.5 nm) exhibiting the charge-transfer channels of the pyridine. The laser fluence was operated at 2 mJ/cm^2 for both complexes.

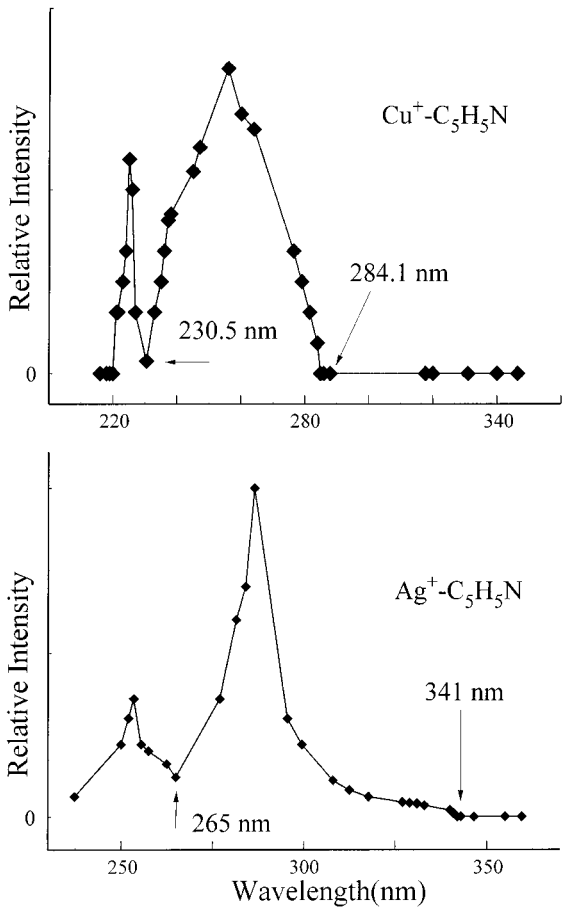

Figure 3. Photodissociation spectra indicating pyridine signal as a function of laser wavelength for $Cu^+-C_5H_5N$ and $Ag^+-C_5H_5N$ complexes. The arrows indicate the thresholds of the absorption bands.

from amplitude of the laser when off, and the depletion signals represent parent ions, as shown in Figure 2. Both complexes revealed the same dissociative behavior with one daughter ion liberated from the parents. The fragment peaks were assigned as pyridine molecules. Although Figure 2 displays fragmentation results at one wavelength for each complex, pyridine$^+$ was the only photoproduct throughout the experiments. It should be noted that both systems investigated here are regarded as *metal cation−pyridine complexes*. It is believed that the positive charge is localized on the metal atoms in the ground states of the complexes because Cu and Ag have lower ionization potentials than that of pyridine. The IP values are 7.72 eV for Cu, 7.57 eV for Ag, and 9.25 eV for C_5H_5N. Studies from previous results, e.g., Ca^+−rare gas,[26] Ag^+−benzene,[10,11] Co^+−CO_2,[27] using the molecular beam method provided this evidence. In fact, our calculations confirmed that this binding feature is composed of mainly electrostatic forces in Cu^+−pyridine and Ag^+−pyridine. Therefore, the photodissociative action induced intramolecular ligand-to-metal charge transfer for pyridine complexes containing Cu^+ and Ag^+.

By inspection of the threshold of the charge-transfer appearance, valuable binding energies can be obtained for the ground states of the complexes along the metal−ligand coordinate. During the signal search, the parent ions were kept stable and the intensity was maintained to be as constant as possible. To avoid a multiphoton process, it was necessary to consider using low laser power. A fragment power dependence showed that one-photon absorption was obtained in the region of the laser fluence used throughout the experiments. The photodissociation spectra of Cu^+−pyridine and Ag^+−pyridine are depicted in Figure 3. Pyridine channels were continuously detected over the region where the energy ranges were 220−284.1 and 237−341 nm for copper ion and silver ion complexes, respectively. Continuous detailed scans were not performed for the whole spectra, whereas the spectral region from 282 to 285 nm for $Cu^+-C_5H_5N$ and wavelengths of 295−300 and 340−343 nm for $Ag^+-C_5H_5N$ were scanned by tuning a dye laser. The spectral resolution of scanning was 0.9 cm^{-1}. Both spectra are structureless and are located at the UV region, as shown in Figure 3. The accuracy of each data point representing pyridine intensities was ±6% or better. These data were accumulated from two to three individual measurements, and the average was taken. It is interesting that both complexes exhibited two absorption bands for the charge-transfer process, while one absorption band in a spectrum covering the visible to UV wavelengths was found for Ag^+−benzene.[10,11] Cu^+ and Ag^+ have similar electronic states. They might, therefore, appear to be analogous with respect to dissociative behavior. The thresholds of the two absorption bands were determined to be at 284.1 and 230.5 nm for Cu^+−pyridine and at 341 and 265 nm for $Ag^+-C_5H_5N$.

Although the detailed excited states of the complexes are not available, it is still important to consider the dissociative processes. The possible mechanisms are discussed by referring to Figure 4. In Figure 4, the well depths of the ground states were acquired from the level of MP2 calculations and the arrows of each energy diagram represent vertical excitations for two onset values. For both complexes, the first reasonable assumption is that the lower energy bands correlate to the Cu (^{2}S) + $C_5H_5N^+$ and Ag (^{2}S) + $C_5H_5N^+$ of the charge-transfer states. The asymptotes of these two charge-transfer states are 35.3 kcal/

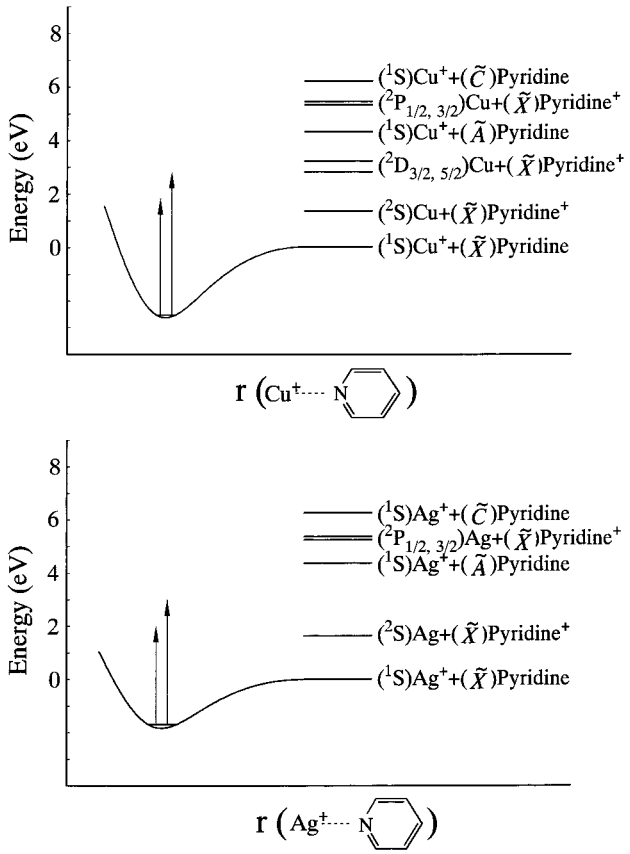

Figure 4. Energy level diagrams showing the asymptote states corresponding to the metal atoms and pyridine molecule. The ground-state potential depths are 2.51 and 1.71 eV, which were calculated at the MP2 level, for Cu^+-pyridine and Ag^+-pyridine, respectively. The arrows represent the thresholds of two structureless absorption bands in each complex.

mol (1.53 eV) and 39 kcal/mol (1.69 eV), calculated from the ionization potential differences of metal atoms and the pyridine molecule, above the atomic states that make up the complex ground states. On the basis of Figures 3 and 4, the energies of both lower energy bands are located above the dissociation limit of those two states. The observation of the pyridine fragments is attributable to the excess of energy over the dissociation limits of the charge-transfer band through the absorption of the photon energies of the complexes. With respect to Ag^+-pyridine, the threshold of the Cu^+-pyridine is blue-shifted by about 16.6 kcal/mol (0.72 eV). This would have reflected the stronger $Cu^+-C_5H_5N$ bond strength by consideration of the onsets and ΔIPs for both complexes. The charge-transfer excited state has a delocalized charge over the pyridine molecule; thus, binding will be involved in polarizing the metal atom from the pyridine ion. The interactions of the excited states should be stronger in $Cu-C_5H_5N^+$ than in $Ag-C_5H_5N^+$ because of the smaller size of Cu. (Cu and Ag have similar polarizabilities.[19]) This result can probably explain why the contour of the first absorption band sharply increased after reaching the threshold in Cu^+-pyridine but gradually increased in Ag^+-pyridine because of the Franck−Condon factor. Analysis of the second maxima at higher energies is more complicated. As can be seen in Figure 4, several excited states are capable of inducing the process by excitation of the solvated metal ions or pyridine chromophore. The pyridine molecule has the allowed electronic n $\rightarrow \pi^*$ transition ($\tilde{A}^1B_1 \leftarrow \tilde{X}^1A_1$) beginning at 287 nm.[28] Formation of $C_5H_5N^+$ is possible by excitation of the solvated pyridine followed by dissociation via electronic curve crossing to the Ag (^{2}S) + $C_5H_5N^+$ asymptote. This procedure will shift the n $\rightarrow \pi^*$ transition of the pyridine to the blue about 2984 cm^{-1} (8.5 kcal/mol; 0.37 eV), which indicates weaker binding in the excited state than in the ground state if the threshold value is the origin of the vertical excitation. With the same chromophore absorption to $Cu^+-C_5H_5N$, the Cu^+ (^{1}S) + C_5H_5N ($\tilde{A}^1$B) surface will be blue-shifted 8630 cm^{-1} (24.7 kcal/mol; 1.07 eV). However, an interesting mechanism involves exciting the complex to the dissociation limit of the second charge-transfer state correlating to Cu (^{2}D) + $C_5H_5N^+$ for the higher structureless band in Cu^+-pyridine, while there is no low-energy ^{2}D state of the Ag atom in Ag^+-pyridine energy levels.[29] This atomic state is 67.3 kcal/mol (2.92 eV) above the asymptote of the ground state. Combining the binding energy (57.9 kcal/mol; 2.51 eV) of the ground state, obtained from calculations, has given 125.2 kcal/mol (5.43 eV) excitation energy to the dissociation limit. The threshold (124.1 kcal/mol; 5.38 eV) of the higher energy band of $Cu^+-C_5H_5N$ thus is almost exactly on the dissociation limit.

It is possible that the excitation of the pyridine chromophore has produced those absorption bands. The lower energy bands of both complexes have contributions from the excitation of the solvated pyridine. In this case, the electronic transitions will be slightly blue-shifted 403 cm^{-1} (1.2 kcal/mol; 0.05 eV) in Cu^+-pyridine and red-shifted 5404 cm^{-1} (15.5 kcal/mol; 0.67 eV) in Ag^+-pyridine relative to the pyridine absorption (n $\rightarrow \pi^*$). The second maximum absorption bands can be attributed to the absorption of the pyridine $\pi \rightarrow \pi^*$ transition ($\tilde{C}^1A_1 \leftarrow \tilde{X}^1A_1$), which starts at 200 nm.[28] The resulting excitation followed by dissociation through a repulsive surface to the metal (^{2}S) + $C_5H_5N^+$ yields the pyridine ions. In this way, the interactions of the excited states relative to second absorption bands of both complexes are all stronger than those of the ground states. The solvating energies are at least 18.9 kcal/mol (0.82 eV) and 34.6 kcal/mol (1.5 eV) for $Cu^+-C_5H_5N$ and $Ag^+-C_5H_5N$, respectively. However, it would be surprising that the excited state of the Ag^+-pyridine has such a significant shift.

The spectral coverage has indeed reflected the efficiency of the charge-transfer process for both complexes. This process is dependent on the Franck−Condon integrals between the ground and excited states and the electronic state density of the excitation energy region. Both complexes exhibit smaller intensity for the higher energy bands. One reason is that the competition of the other process has lessened the charge-transfer efficiency because of the greater number of electronic states in the higher energy region.

In summary, two absorption bands were observed in each complex. However, the dissociative mechanism may not be quite the same for either species. It is possible that $Cu^+-C_5H_5N$ owns the second charge-transfer state at the lower energy.

Geometries and Binding Energies. Although it is not clear whether the lower energy structureless band is a charge-transfer electronic transition or a process through the absorption of the solvated pyridine, the upper boundary of the binding energy of the ground state can be deduced from the absorption threshold and the IP difference of the metal and C_5H_5N using the following procedure:

$$h\nu \geq D_0'' + \Delta\mathrm{IP}$$

On the basis of the above equation, the binding energies were derived to be 65.5 kcal/mol on Cu^+-pyridine and 45.2 kcal/mol on Ag^+-pyridine. It is apparent that Cu^+ is more strongly bound to the pyridine than is Ag^+. From the electrostatic

TABLE 1: Geometrical Parameters (Å and deg) of Pyridine Complexes Containing Cu^+ and Ag^+ Predicted by Theoretical (MP2/(HW(f), 6-31G(d,p))) and Experimental Values of Pyridine

	Cu^+−pyridine	Ag^+−pyridine	pyridine (calcd)[a]	pyridine (exptl)[b]
$r(M^+-N)$	1.946	2.196		
r(C1−N)[c]	1.380	1.379	1.372	1.340
r(C1−C2)[c]	1.404	1.406	1.410	1.395
r(C2−C3)[c]	1.412	1.411	1.412	1.394
∠C1−N−C5[c]	118.9	118.3	117.1	116.8
∠N−C1−C2[c]	121.7	122.1	123.2	123.9
∠C1−C2−C3[c]	119.4	119.3	118.9	118.5
∠C2−C3−C4[c]	118.9	118.8	118.7	118.3

[a] Structure optimized at MP2/6-31G(d,p). [b] Taken from ref 19. [c] The numbering refers to Figure 5.

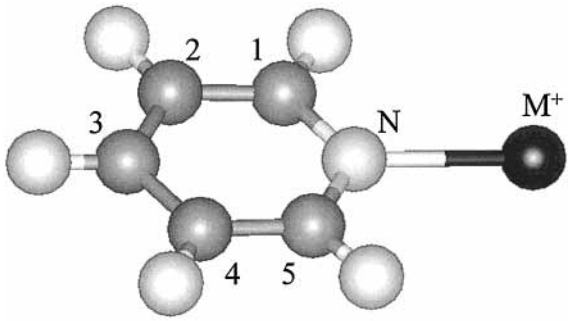

C_{2v} symmetry

Figure 5. Geometry of the M^+−pyridine complex, where $M^+ = Cu^+$ or Ag^+.

(charge−dipole) point of view, the smaller copper metal is expected to have larger binding energy. Compared with Ag^+−pyridine, Ag^+−benzene with primary ion-induced dipole forces has less binding (35.5 kcal/mol),[10,11] obtained from the same experimental technique. To fully understand the geometries and interactions of the pyridine complexes, theoretical calculations were performed on group IB (Cu^+ and Ag^+)−pyridine systems.

Three calculation methods, i.e., HF, MP2, and B3LYP, and several basis sets were used to optimize the structures. The results are shown in Table 1. All calculations predicted C_{2v} symmetry for the two complexes, as illustrated in Figure 5. We optimized our complexes within C_s symmetry, where the metal atoms are allowed to move out of the pyridine plane. It turned out that these optimizations ended up with the C_{2v} minima. The metal ions point toward the nitrogen atom and have slight distortion on the pyridine structure. The structural data in Table 1 were obtained from MP2/(HW(f),6-31G(d,p)), where the Hay−Wadt basis augmented with f polarization was denoted as HW(f) for metals.

We chose Ag^+−pyridine as an example to show the effects of the computational method and the basis set calculation choice. Increasing the basis sets caused reduction of the binding energies. The significant decrease in D_e values was found by changing the basis from 6-31G to 6-31G(d). In fact, the computations with 6-31G on C, H, and N atoms tended to have the strongest metal-to-ligand interactions. This probably originates from the basis set superposition error (BSSE). From the results of the Table 2, the diffuse functions added to heavy atoms and p polarization functions added to hydrogen atoms have little influence on the binding energies. At the HF and B3LYP levels, the f polarization functions in the HW basis had a small effect,

TABLE 2: Binding Energies (kcal/mol) and Ag^+−N Bond Distances (Å) as a Function of Methods and Basis Sets for Ag^+−Pyridine Complex

method	basis set	D_e	D_0	$r(Ag^+-N)$
	[HW,6-31G][a]	40.3	39.4	2.282
	[HW(f),6-31G]	40.7	40.0	2.275
HF	[HW(f),6-31+G]	40.0		2.278
	[HW(f),6-31G(d)]	35.5	34.7	2.311
	[HW(f),6-31G(d,p)]	35.8	35.0	2.311
	[HW,6-31G][a]	47.2		2.232
MP2	[HW(f),6-31G]	50.5	49.8	2.196
	[HW(f),6-31G(d)]	40.4		2.198
	[HW(f),6-31G(d,p)]	40.0	39.3	2.198
B3LYP	[HW,6-31G][a]	50.0		2.172
	[HW(f),6-31G]	50.5	49.9	2.165
	[HW(f),6-31+G]	51.2		2.179
	[HW(f),6-31G(d)]	42.6		2.192
	[HW(f),6-31G(d,p)]	42.5	41.9	2.190

[a] HW RECP basis without f polarization functions for silver.

TABLE 3: Binding Energies (kcal/mol) and Metal Cation−N Bond Distances (Å) at Three Methods for Each Complex

complex	method	D_e	D_0	$r(M^+-N)$
Cu^+−pyridine	HF/[HW(f),6-31G(d,p)]	50.2	49.0	2.049
	MP2/[HW(f),6-31G(d,p)]	58.8	57.8	1.940
	B3LYP/[HW(f),6-31G(d,p)]	66.5	65.4	1.931
Ag^+−pyridine	HF/[HW(f),6-31G(d,p)]	35.8	35.0	2.311
	MP2/[HW(f),6-31G(d,p)]	40.0	39.3	2.198
	B3LYP/[HW(f),6-31G(d,p)]	42.5	41.9	2.190

but the bond strength was enhanced by the MP2 method. This observation is consistent with the previous studies of Ag^+−benzene.[7]

The basis set with 6-31G(d,p) was used to display M^+−pyridine bond distance and binding energies, as depicted in Table 3. As we can see, the HF level predicted the lowest bond strength while B3LYP calculated the strongest binding for each complex. MP2 predicted binding energies are close to those obtained by B3LYP. From all of the methods applied, the order of the interactions between metal cations and pyridine is the following:

$$Ag^+-C_5H_5N < Cu^+-C_5H_5N$$

Compared with the experimental values, the B3LYP level of theory has the closest estimation, particularly in the case of Cu^+−pyridine. The experimental values are consistently larger than those (D_0) estimated from three different methods. In general, the photodissociative measurements of this study are expected to yield an upper limit of the binding energy unless the dissociative behavior takes place near or at dissociation limit of a state. As mentioned earlier, if the lowest energy band observed belongs to charge-transfer state, this excited state will have weaker strength than the ground state on the basis of the electrostatic model; the binding energy is expected to be overestimated experimentally. On the basis of the recognition of the MP2 and B3LYP performance in other systems, it has been shown that the hybrid functional (B3LYP) has a tendency to overestimate the interaction energy more severely than the MP2.[30] From the earlier discussion, the higher energy band of the $Cu^+-C_5H_5N$ possibly corresponds to the second charge-transfer state. If so, the subtraction of ΔIP from threshold results in 56.7 kcal/mol of binding strength, which is only 1 kcal/mol less than the prediction of the MP2 level. Overall, other experimental techniques, such as collision-induced dissociation, can definitely provide alternative information with respect to

bond strength. Compared to the binding energies of benzene complexes, Bauschlicher and co-workers have calculated ground-state dissociation energies of 51.1 and 36.5 kcal/mol for $Cu^+-C_6H_6$ and $Ag^+-C_6H_6$, respectively.[31] The interactions of metal ions with ligands are charge-induced dipoles in benzene complexes and charge−dipole interactions in pyridine complexes.

Natural bond orbital (NBO) analysis was performed on the complexes containing Cu^+ and Ag^+ at the MP2 level as well. The charges on metal ions are $Cu^+(0.89)$ and $Ag^+(0.94)$. It is known that the group IB ions with singly positive charges have electronic configurations of the ground states as $d^{10}s^0$. Occupancies of the valence s orbitals are found to be 0.17 (4s) for Cu^+ and 0.07 (5s) for Ag^+. There is very little electron transfer from C_5H_5N to Cu^+ cations. The population of the d_{z^2}, which is the highest occupied atomic orbital, of the metal cations revealed that $Cu^+(1.92)$ and $Ag^+(1.96)$ are essentially doubly occupied. These observations suggest that bonding between Cu^+ and Ag^+ and pyridine are mainly electrostatic.

In summary, theoretical calculations have shown that Cu^+ and Ag^+ atoms interact with the nitrogen of the pyridine molecule. The binding is dominated by electrostatic charge−dipole forces in both complexes.

Conclusions

Pyridine, an aromatic species other than benzene, combined with Cu^+ or Ag^+ displayed dissociative charge-transfer reaction. The energy ranges of this behavior are 220−284.1 and 237−341 nm for Cu^+−pyridine and Ag^+−pyridine, respectively. For this study, pyridine complexes should have been good candidates for investigation of the vibronic structure originating from the pyridine chromophore. Unfortunately, continuous structureless bands were observed for both complexes. On the basis of the theoretical results, $Cu^+-C_5H_5N$ and $Ag^+-C_5H_5N$ exhibited electrostatic interactions in binding and C_{2v} symmetry in structure.

Acknowledgment. This work was supported by the National Science Council of the Republic of China. We thank the National Center for High-Performance Computing for computer time and facilities.

References and Notes

(1) Sauer, J. *Chem. Rev.* **1989**, *89*, 199.
(2) Bäckvall, J.-E.; Bökman, F.; Blomberg, M. R. A. *J. Am. Chem. Soc.* **1992**, *114*, 534.
(3) Dougherty, D. A. *Science* **1996**, *271*, 163.
(4) Szilagyi, R. K.; Frenking, G. *Organometallics* **1997**, *16*, 4807.
(5) Bauschlicher, C. W.; Partridge, H.; Langhoff, S. R. *J. Phys. Chem.* **1992**, *96*, 3273.
(6) Luna, A.; Amekraz, B.; Tortajada, J. *Chem. Phys. Lett.* **1997**, *266*, 31.
(7) Ma, N. L.; Ng, K. M.; Tsang, C. W. *Chem. Phys. Lett.* **1997**, *277*, 306.
(8) Nicholas, N. J.; Hay, B. P.; Dixon, D. A. *J. Phys. Chem. A* **1999**, *103*, 1394.
(9) Henson, N. J.; Hay, P. J.; Redondo, A. *Inorg. Chem.* **1999**, *38*, 1618.
(10) Willey, K. F.; Cheng, P. Y.; Bishop, M. B.; Duncan, M. A. *J. Am. Chem. Soc.* **1991**, *113*, 4721.
(11) Willey, K. F.; Yeh, C. S.; Robbins, D. L.; Duncan, M. A. *J. Phys. Chem.* **1992**, *96*, 9106.
(12) Jarrold, M. F.; Misev, L.; Bowers, M. T. *J. Chem. Phys.* **1984**, *81*, 4369.
(13) Masnovi, J. M.; Kochi, J. K. *J. Am. Chem. Soc.* **1985**, *107*, 6781.
(14) Dixon-Warren, St. J.; Polanyi, J. C.; Stanners, C. D.; Xu, G. Q. *J. Phys. Chem.* **1990**, *94*, 5664.
(15) Spence, T. G.; Trotter, B. T.; Burns, T. D.; Posey, L. A. *J. Phys. Chem. A* **1998**, *102*, 6101.
(16) Weis, P.; Kemper, P. R.; Bower, M. T. *J. Phys. Chem. A* **1997**, *101*, 8207.
(17) Holland, P. M.; Castleman, A. W. *J. Chem. Phys.* **1982**, *76*, 4195.
(18) Mulliken, R. S. *J. Am. Chem. Soc.* **1952**, *64*, 811.
(19) Lide, D. R. *CRC Handbook of Chemistry and Physics*, 79th ed.; CRC Press: London, 1998.
(20) Yang, Y. S.; Yeh, C. S. *Chem. Phys. Lett.* **1999**, *305*, 395.
(21) Bauschlicher, C. W.; Partridge, H. *Chem. Phys. Lett.* **1991**, *181*, 129.
(22) Lu, W.; Yang, S. *J. Phys. Chem. A* **1998**, *102*, 825.
(23) Hay, P. J.; Wadt, W. R. *J. Chem. Phys.* **1985**, *82*, 299.
(24) Ehlers, A. W.; Böhme, M.; Dapprich, S.; Gobbi, A.; Höllwarth, A.; Jonas, V.; Köhler, K. F.; Stegmann, R.; Veldkamp, A.; Frenking, G. *Chem. Phys. Lett.* **1993**, *208*, 111.
(25) Frisch, M. J.; Trucks, G. W.; Schlegel, H. B.; Scuseria, G. E.; Robb, M. A.; Cheeseman, J. R.; Zakrzewski, V. G.; Montgomery, J. A., Jr.; Stratmann, R. E.; Burant, J. C.; Dapprich, S.; Millam, J. M.; Daniels, A. D.; Kudin, K. N.; Strain, M. C.; Farkas, O.; Tomasi, J.; Barone, V.; Cossi, M.; Cammi, R.; Mennucci, B.; Pomelli, C.; Adamo, C.; Clifford, S.; Ochterski, J.; Petersson, G. A.; Ayala, P. Y.; Cui, Q.; Morokuma, K.; Malick, D. K.; Rabuck, A. D.; Raghavachari, K.; Foresman, J. B.; Cioslowski, J.; Ortiz, J. V.; Stefanov, B. B.; Liu, G.; Liashenko, A.; Piskorz, P.; Komaromi, I.; Gomperts, R.; Martin, R. L.; Fox, D. J.; Keith, T.; Al-Laham, M. A.; Peng, C. Y.; Nanayakkara, A.; Gonzalez, C.; Challacombe, M.; Gill, P. M. W.; Johnson, B. G.; Chen, W.; Wong, M. W.; Andres, J. L.; Head-Gordon, M.; Replogle, E. S.; Pople, J. A. *Gaussian 98*, revision A.3; Gaussian, Inc.: Pittsburgh, PA, 1998.
(26) Pullins, S. H.; Scurlock, C. T.; Reddic, J. E.; Duncan, M. A. *J. Chem. Phys.* **1996**, *104*, 7518.
(27) Bellert, D.; Buthelezi, T.; Brucat, P. J. *Chem. Phys. Lett.* **1998**, *290*, 316.
(28) Herzberg, G. *Electronic Spectra and Electronic Structure of Polyatomic Molecules*; Van Nostrand Reinhold: New York, 1996.
(29) Moore, C. E. *Atomic Energy Levels*; National Bureau of Standards: Washington, DC, 1971.
(30) Hoyau, S.; Ohanessian, G. *Chem. Phys. Lett.* **1997**, *280*, 266.
(31) Bauschlicher, C. W.; Partridge, H.; Langhoff, S. R. *J. Phys. Chem.* **1992**, *96*, 3273.